

# Postdetection Switch-and-Stay Diversity in Rician Fading

Sasan Haghani, *Student Member, IEEE*, and Norman C. Beaulieu, *Fellow, IEEE*

Department of Electrical and Computer Engineering, University of Alberta, Edmonton, Alberta, Canada, T6G 2V4

E-mail: haghani@ece.ualberta.ca, beaulieu@ece.ualberta.ca

**Abstract**—Recent work has examined the performances of dual branch postdetection switch-and-stay combining (SSC) for noncoherent binary orthogonal frequency-shift keying (BFSK) and noncoherent  $M$ -ary orthogonal frequency-shift keying (MFSK) operating in the presence of slow, flat fading modeled by Rayleigh, Nakagami- $m$ , and Rician distributions. These studies are important, in particular, because they quantify the improvement of postdetection SSC over predetection SSC. However, previous work on the performance of postdetection SSC over Rician fading is incorrect. In this paper, we present correct analyses of the bit error rate (BER) performance of BFSK and MFSK with dual-branch postdetection SSC in Rician fading. Extensive Monte Carlo simulations are carried out to verify the validity of the analytical results. Our results show that the performance gain of postdetection SSC over predetection SSC is much less than previously reported.

**Keywords**—Diversity combining, fading channels, postdetection diversity, predetection diversity, switch-and-stay combining.

## I. INTRODUCTION

In two recent *Transactions* papers, [1],[2], the performances of dual-branch postdetection switch-and-stay combining (SSC) for noncoherent orthogonal binary frequency-shift keying (BFSK) and noncoherent orthogonal  $M$ -ary frequency-shift keying (MFSK) in Rayleigh, Nakagami- $m$  and Rician fading channels are studied. These papers quantify the performance gain of postdetection SSC over predetection SSC and show that postdetection SSC outperforms predetection SSC by several dBs in signal-to-noise ratio (SNR) for a given bit error rate (BER). In this paper, we show that the previous analyses of BFSK and MFSK with dual-branch postdetection SSC in Rician fading are mathematically inaccurate and we derive correct BER expressions for the performances of these systems. The correctness of our analytical results are supported by extensive Monte Carlo simulations. Using our accurate analytical results, we obtain optimum switching thresholds that minimize the BER performances of dual-branch BFSK and MFSK with postdetection SSC in Rician fading. Furthermore, we show that the performance gain of postdetection SSC over predetection SSC is over-estimated in [1],citeS2 by several dBs in SNR for a given BER in Rician fading.

The remainder of this paper is organized as follows. In Section II, we derive analytical results for the performance of BFSK with postdetection SSC in Rician fading. These results are used to obtain optimum switching thresholds that minimize the BER of BFSK with postdetection SSC. In section MFSKsection, previous analyses on the performance of MFSK with postdetection SSC in Rician fading, are corrected. In each section, mathematical and simulation results are used to verify our analyses and numerical examples are provided to compare the performances of postdetection and predetection SSC. Finally, some conclusions are given in Section IV.

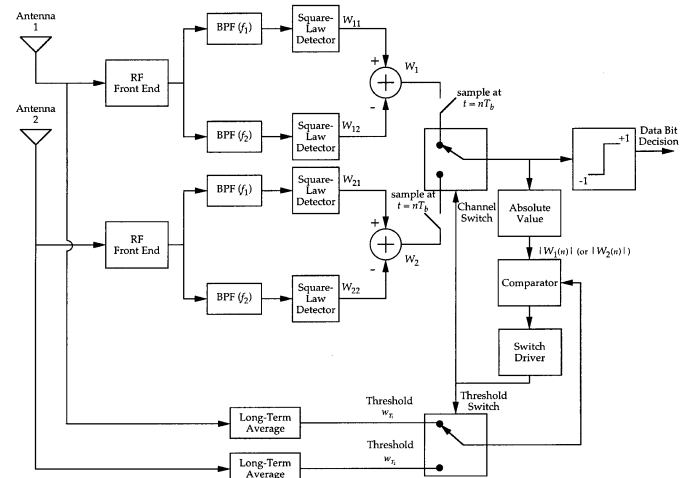


Fig. 1. Block diagram of noncoherent BFSK with postdetection SSC (after [1, Fig. 1]).

## II. ERROR RATE OF BFSK WITH POSTDETECTION SSC

A block diagram of a BFSK system with postdetection SSC is given in Fig. 1 (after [1, Fig. 1]). The switching mechanism and the considerations involving the selection of an optimum switching threshold are discussed in detail in [1, Section III]. In the following, we only summarize the essential material that is relevant to the development of the current paper. The reader is referred to [1] for more details. Our notations closely follow the notations used in [1].

### A. Switch-and-Stay Diversity

Let  $|W_1(n)|$  and  $|W_2(n)|$  denote the amplitude of the RVs  $W_1$  and  $W_2$  at time  $t_n = nT_b$ . Assume, without loss of generality, that the switch is connected to antenna one. The switch will remain connected to antenna one, for the next  $T_b$  seconds, as long as  $|W_1(n)| > w_{T_1}$ , where  $w_{T_1}$  is a predetermined switching threshold. Note that the decision to remain connected to antenna one does not depend on the situation on antenna two. The system will switch to antenna two if  $|W_1(n)| < w_{T_1}$ . A similar statement holds if the switch is connected to antenna two. In mathematical terms the switching decision can be written as

$$W(n) = W_i(n) \quad \text{if} \quad \begin{cases} W(n-1) = W_i(n-1) & \text{and} \\ |W_i(n)| \geq w_{T_i} & \\ \text{or} & \\ W(n-1) = W_{\bar{i}}(n-1) & \text{and} \\ |W_{\bar{i}}(n)| \leq w_{T_{\bar{i}}} & \end{cases} \quad (1)$$

where  $i = 1, 2$  and  $\bar{i}$  denotes the 2's complement of  $i$ .

A general expression for the average bit error rate of BFSK with postdetection SSC is given in [1, Section IV] and is not repeated here for the sake of brevity. For the case of independent and identically (i.i.d) branches this BER expression reduces to

$$F_W(-w_T) + [F_W(w_T) - F_W(-w_T)]F_W(0) \quad (2)$$

where  $F_W(\cdot)$  is the cumulative distribution function (CDF) of  $W_i$ ,  $i = 1, 2$  and  $w_T$  is the switching threshold.

### B. Error Rate Analysis in Rician Fading

In [1], the authors have derived an incorrect CDF for  $W_1$  and  $W_2$  and as a result their analysis in [1, Section VI.A] is incorrect. In the following, we correct the results of [1, Section VI.A] and derive correct expressions for the BER of postdetection SSC in Rician fading.

Similar to [1], and without loss of generality, we assume that the symbol corresponding to  $f_1$  is transmitted and the switch is connected to antenna one. Then, the RV  $W_{11}$  can be written as  $W_{11} = |2E_b\alpha_1 e^{j\theta_1} + N_{11}|^2$  where  $\alpha_1 e^{j\theta_1}$  is the complex fading gain on channel one and  $N_{11}$  is a zero-mean complex Gaussian RV with variance  $\sigma^2 = 2E_b N_0$ . To proceed, we expand  $W_{11}$  as  $W_{11} = |2E_b X_1 + N_1^I|^2 + |2E_b X_2 + N_1^Q|^2$  where  $X_1$  and  $X_2$  is Gaussian RV with mean  $m_1$  and  $m_2$  and variance  $\sigma_x^2$  and  $N_1^I$  and  $N_1^Q$  is zero-mean, Gaussian RV with variance  $\sigma^2 = 2E_b N_0$ , respectively. To find the correct distribution of  $W_{11}$  we first relate the Rice factor,  $K_1$ , to parameters  $m_1$  and  $m_2$  using [3] as  $K_1 = \frac{m_1^2 + m_2^2}{2\sigma_x^2}$ . Then, one can show that  $W_{11}$  is a non-central chi-squared random variable with non-centrality parameters  $s^2 = \frac{4E_b N_0 K \bar{\gamma}_1}{K+1}$  and variance  $\sigma_1^2 = 2E_b N_0 \frac{\bar{\gamma}_1 + K + 1}{K+1}$ . Therefore, the CDF of  $W_{11}$  is given by

$$F_{W_{11}}(w) = 1 - Q_1 \left( \sqrt{P_1(K_1, \bar{\gamma}_1)}, \sqrt{\frac{P_2(K_1, \bar{\gamma}_1)w}{4E_b N_0}} \right) \quad (3a)$$

where  $Q_1(\cdot, \cdot)$  denotes the Marcum-Q function defined in [4] and  $P_1(K, \bar{\gamma})$  and  $P_2(K, \bar{\gamma})$  are given by

$$P_1(K, \bar{\gamma}) = \frac{2K\bar{\gamma}}{\bar{\gamma} + K + 1}, \quad P_2(K, \bar{\gamma}) = \frac{2(K+1)}{(\bar{\gamma} + K + 1)}. \quad (3b)$$

The RV  $W_{12} = |2E_b N_{12}|^2$  is a central chi-squared RV with variance  $\sigma^2 = 2E_b N_0$ . Thus, its CDF is given as

$$F_{W_{22}}(w) = 1 - \exp \left( -\frac{w}{4E_b N_0} \right). \quad (4)$$

An analytical expression for the CDF of the difference between a noncentral chi-square RV and a central chi-square RV is given in [1, eq. (51)]. Using [1, eq. (51)] we derive the CDF of  $W_1$ , after some mathematical simplifications, as

$$F_{W_1}(w) = \begin{cases} Y_1(K_1, \bar{\gamma}_1) \exp \left( \frac{w}{4E_b N_0} \right), & w < 0 \\ 1 - Q_1 \left( \sqrt{P_1(K_1, \bar{\gamma}_1)}, \sqrt{\frac{P_2(K_1, \bar{\gamma}_1)w}{4E_b N_0}} \right) \\ + Y_1(K_1, \bar{\gamma}_1) \exp \left( \frac{w}{4E_b N_0} \right) \\ \times Q_1 \left( \sqrt{Y_2(K_1, \bar{\gamma}_1)}, \sqrt{\frac{Y_3(K_1, \bar{\gamma}_1)w}{4E_b N_0}} \right), & w > 0 \end{cases} \quad (5a)$$

where

$$Y_1(K, \bar{\gamma}) = \frac{K+1}{2K+2+\bar{\gamma}} \exp \left( -\frac{\bar{\gamma}K}{2K+2+\bar{\gamma}} \right) \quad (5b)$$

$$Y_2(K, \bar{\gamma}) = \frac{2\bar{\gamma}K(K+1)}{(\bar{\gamma}+K+1)(\bar{\gamma}+2+2K)} \quad (5c)$$

$$Y_3(K, \bar{\gamma}) = \frac{2(\bar{\gamma}+2+2K)}{\bar{\gamma}+K+1}. \quad (5d)$$

Note that (5) corrects [1, eq. (35)]. If the switch is connected to antenna 2, then going through the same steps, one obtains the CDF of  $W_2$  which is equal to the expression given in (5), except that  $K_1$  and  $\bar{\gamma}_1$  should be replaced with  $K_2$  and  $\bar{\gamma}_2$ , respectively. Substituting the CDFs of  $W_1$  and  $W_2$  in the general expression for the BER given in [1, Section III], one obtains the BER of noncoherent BFSK with postdetection SSC in Rician fading. In the case of i.i.d branches the average BER reduces to

$$P_b(E) = Y_1(K, \bar{\gamma}) \left[ \exp \left( -\frac{\eta_T \bar{\gamma}}{4} \right) + 1 - Q_1 \left( \sqrt{P_1(K, \bar{\gamma})}, \sqrt{\frac{\eta_T \bar{\gamma} P_2(K, \bar{\gamma})}{4}} \right) + Y_1(K, \bar{\gamma}) \exp \left( \frac{\eta_T \bar{\gamma}}{4} \right) \times \left( Q_1 \left( \sqrt{Y_2(K, \bar{\gamma})}, \sqrt{\frac{Y_3(K, \bar{\gamma}) \bar{\gamma} \eta_T}{4}} \right) - \exp \left( -\frac{\bar{\gamma} \eta_T}{2} \right) \right) \right] \quad (6)$$

where  $\eta_T$  is the normalized switching threshold. Note that (6) corrects [1, eq. (37)]. For  $K = 0$ , which corresponds to a Rayleigh fading model, using  $Q_1(0, b) = \exp \left( -\frac{b^2}{2} \right)$ , one can show that (6) reduces to

$$P_b(E) = \frac{1}{\bar{\gamma} + 2} \times \left( 1 + \frac{1 + \bar{\gamma}}{2 + \bar{\gamma}} \left[ \exp \left( -\frac{\eta_T \bar{\gamma}}{4} \right) - \exp \left( -\frac{\eta_T \bar{\gamma}}{4(1 + \bar{\gamma})} \right) \right] \right) \quad (7)$$

which is equal to [1, eq. (19)], as expected.

### C. Theoretical and Simulation Results

We have conducted several Monte Carlo simulations to assess the validity of our analytical results. Fig. 3 shows the BER performance of postdetection SSC in i.i.d Rician fading for  $K = 0, 3$  and 6 obtained from the theoretical expressions

given in (6) and [1, eq. (37)] and also from Monte Carlo simulations. Fig. 3 shows excellent agreement between the simulation and analytical result obtain in (6). Fig. 3 also shows that the expression given in [1, eq. (37)] is only valid for  $K = 0$  which corresponds to i.i.d Rayleigh fading. For other values of  $K$  and for a given BER, the expression given in [1, eq. (37)] overestimates the BER of BFSK with postdetection SSC by several dBs in SNR. For example, at a BER of  $10^{-3}$  and for  $K = 3$ , the difference between the correct result and the incorrect result is 0.7 dB and at a BER of  $10^{-4}$  and for  $K = 6$ , the difference between the correct result and the incorrect result is 1.3 dB.

Fig. 4 shows the BER performance of BFSK with postdetection SSC in i.i.d Rician fading for  $K = 6$  and for several values of average SNR. The optimal switching thresholds are indicated in the figure. Note that as the average SNR increases, the optimal switching threshold decreases. This implies that in better channel conditions the system switches more often to exploit the fading conditions on the other channel [2].

Fig. 5 compares the optimal BER performances of predetection SSC with postdetection SSC in i.i.d Rician fading for  $K = 1, 5$  and  $10$ . Fig. 5 shows that as the fading parameter,  $K$ , increases, the performance difference between predetection and postdetection SSC increases. For example, at a BER of  $10^{-3}$  and for  $K = 1, 5$  and  $K = 10$ , the SNR difference between postdetection and predetection SSC is 0.93 dB, 1.17 dB and 1.28 dB, respectively. Fig. 5 also shows that previous results have overestimated the performance improvement of postdetection SSC over predetection SSC by several dBs (refer to [1, Fig. 8]). For example, at a BER of  $10^{-4}$  and for  $K = 5$  and  $K = 10$ , the SNR difference between predetection SSC and postdetection SSC, as shown in Fig. 5 is only 1.30 dB and 2.30 dB, respectively, whereas in [1, Fig. 8] the SNR difference is reported to be 2.30 dB and 3.38 dB, respectively. Fig. 5 corrects [1, Fig. 8].

### III. SER ANALYSIS OF MFSK WITH POSTDETECTION SSC

#### A. Mathematical Model

A block diagram of a MFSK system with dual-branch postdetection SSC is shown in Fig. 2 (after [2, Fig. 1]). The switching mechanism is the same as that explained in Section II-A. A general expression for the average symbol error rate (SER) of noncoherent MFSK with dual-branch SSC is given in [2, eq. (8)] and is not repeated here for the sake of brevity.

#### B. SER Analysis in Rician Fading

The SER expression given in [2, eq. (8)] shows that to calculate the SER one needs to know the PDFs and CDFs of  $W_{ij}, i = 1, 2, j = 1, \dots, M$  as shown in Fig. 2 and defined as  $W_{11} = E_s^2 |2\alpha_1 e^{j\theta_1} + N_{11}|^2, W_{21} = E_s^2 |2\alpha_2 e^{j\theta_2} + N_{21}|^2$  and  $W_{jm} = E_s^2 |N_{jm}|^2, j = 1, 2, m = 2, \dots, M$  where  $\alpha_i e^{j\theta_i}, i = 1, 2$  are the channel gains and  $N_{ij}, i = 1, 2, j = 1, \dots, M$  are zero mean, complex Gaussian RVs with variance  $4N_0/E_b$ . In [2], the authors have correctly assumed that the RVs  $W_{11}$  and  $W_{21}$  are noncentral chi-squared, but with incorrect parameters. Similar to the previous section, we drive the PDF and CDF of  $W_{11}$  and  $W_{21}$  as

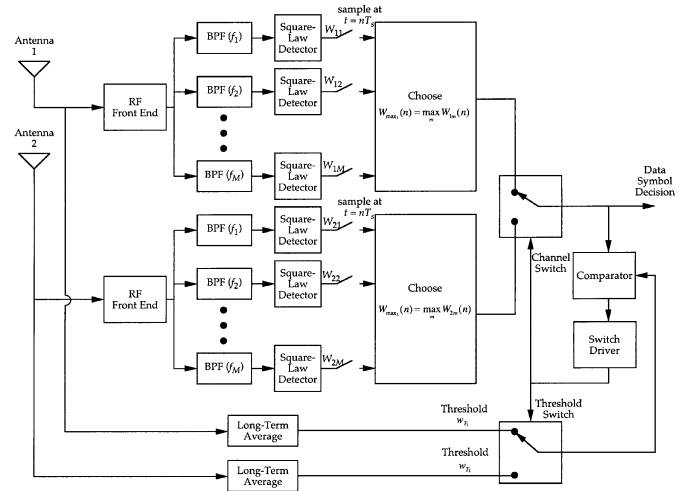


Fig. 2. Block diagram of noncoherent MFSK with postdetection SSC (after [2, Fig. 1]).

$$f_{W_{i1}}(w) = \frac{K_i + 1}{4E_b N_0 (\bar{\gamma}_i + K_i + 1)} \exp\left(-\frac{K \bar{\gamma}_i}{\bar{\gamma}_i + K_i + 1}\right) \times \exp\left(-\frac{(K_i + 1)w}{4E_b N_0 (\bar{\gamma}_i + K_i + 1)}\right) I_0\left(\sqrt{\frac{K_i \bar{\gamma}_i (K_i + 1)w}{E_b N_0 (\bar{\gamma}_i + K_i + 1)^2}}\right) \quad (8)$$

$$F_{W_{i1}}(w) = 1 - Q_1\left(\sqrt{P_1(K_i, \bar{\gamma}_i)}, \sqrt{\frac{P_2(K_i, \bar{\gamma}_i)w}{4E_b N_0}}\right), \quad i = 1, 2. \quad (9)$$

The PDFs and CDFs of  $W_{jm}, j = 1, 2, m = 2, \dots, M$  are

$$f_{W_{jm}}(w) = \frac{\exp\left(-\frac{w}{4E_b N_0}\right)}{4E_b N_0}, \quad j = 1, 2, \quad m = 2, \dots, M \quad (10)$$

$$F_{W_{jm}}(w) = 1 - \exp\left(-\frac{w}{4E_b N_0}\right), \quad j = 1, 2, \quad m = 2, \dots, M. \quad (11)$$

Substituting (8)-(11) in [2, eq. (8)] and after some mathematical manipulations one can obtain a closed-form expression for the SER of MFSK with dual-branch postdetection SSC in Rician fading which corrects [2, eq. (28)]. The procedure, is described below for the case of i.i.d Rician fading in detail. One can show that for i.i.d Rician fading the SER in [2, eq.(8)] reduces to

$$P_s(E) = 1 - \int_{w_t}^{\infty} f_{W_{11}}(x) [F_{W_{12}}(x)]^{M-1} dx - F_{W_{11}}(w_t) [F_{W_{12}}(w_t)]^{M-1} \int_0^{\infty} f_{W_{21}}(x) [F_{W_{22}}(x)]^{M-1} dx. \quad (12)$$

Using (8), (11), [5, eq. (8.445)] and [5, eq. (3.381.3)], assuming that  $K > 0$ , and after some mathematical manipulation and

integral evaluations, the first integral in (12) reduces to

$$\begin{aligned} & \exp\left(-\frac{K\bar{\gamma}_1}{K+\bar{\gamma}_1+1}\right) \sum_{i=0}^{\infty} \sum_{l=0}^{M-1} \frac{K+1}{(K+1)(l+1)+l\bar{\gamma}} \\ & \times \frac{(-1)^l \binom{M-1}{l}}{(i!)^2} \left(\frac{K\bar{\gamma}(K+1)}{(K+1)(l+1)+l\bar{\gamma}}(K+1+\bar{\gamma})\right)^i \\ & \times \Gamma\left(i+1, \frac{\eta_T \bar{\gamma} (K+1)(l+1)+l\bar{\gamma}_1}{4(K+1+\bar{\gamma}_1)}\right) \end{aligned} \quad (13)$$

where  $\eta_T$  is the normalized switching threshold. For  $K=0$ , one can show that the first integral reduces to

$$\sum_{l=0}^{M-1} \frac{(-1)^l}{1+l(1+\bar{\gamma})} \binom{M-1}{l} \exp\left(-\frac{\eta_T \bar{\gamma} (1+l(1+\bar{\gamma}))}{4(1+\bar{\gamma})}\right). \quad (14)$$

To calculate the second integral in (12), we use (8), (11) and [5, eqs. (6.643.2), (9.220.2), (9.215.1)]. The result, after some routine algebra, is

$$\sum_{l=0}^{M-1} (-1)^l \binom{M-1}{l} \frac{(K+1) \exp\left(-\frac{Kl\bar{\gamma}}{l\bar{\gamma}+(K+1)(l+1)}\right)}{l\bar{\gamma}+(K+1)(l+1)} \quad (15)$$

which for  $K=0$  reduces to  $\sum_{l=0}^{M-1} \frac{(-1)^l}{1+l(1+\bar{\gamma})} \binom{M-1}{l}$ .

Now, substituting (9) and (11) in (12), using (13), (14) and (15), and after some re-arranging, we obtain the SER of MFSK with dual branch postdetection SSC as (for  $K > 0$ )

$$\begin{aligned} P_s(E) &= 1 - \sum_{l=0}^{M-1} (-1)^l \binom{M-1}{l} \left\{ \exp\left(-\frac{K\bar{\gamma}_1}{K+\bar{\gamma}_1+1}\right) \right. \\ & \times \sum_{i=0}^{\infty} \frac{1}{(i!)^2} \frac{K+1}{(K+1)(l+1)+l\bar{\gamma}} \left(\frac{K\bar{\gamma}(K+1)}{(K+1)(l+1)+l\bar{\gamma}}\right)^i \times \\ & \Gamma\left(i+1, \frac{\eta_T \bar{\gamma} (K+1)(l+1)+l\bar{\gamma}_1}{4(K+1+\bar{\gamma}_1)}\right) + \frac{K+1}{l\bar{\gamma}+(K+1)(l+1)} \\ & \times \exp\left(-\frac{Kl\bar{\gamma}}{l\bar{\gamma}+(K+1)(l+1)}\right) \left(1 - \exp\left(-\frac{\eta_T \bar{\gamma}}{4}\right)\right)^{M-1} \\ & \left. \times \left(1 - Q_1\left(\sqrt{\frac{2K\bar{\gamma}}{\bar{\gamma}+K+1}}, \sqrt{\frac{\eta_T \bar{\gamma} (K+1)}{2(\bar{\gamma}+K+1)}}\right)\right)\right\} \end{aligned} \quad (16a)$$

and for  $K=0$  as

$$\begin{aligned} P_s(E) &= \sum_{l=0}^{M-1} \frac{(-1)^l \binom{M-1}{l}}{1+l(1+\bar{\gamma})} \left\{ \exp\left(-\frac{Kl\bar{\gamma}}{l\bar{\gamma}+(K+1)(l+1)}\right) \right. \\ & \left. - \left(1 - \exp\left(-\frac{\eta_T \bar{\gamma}}{4(1+\bar{\gamma})}\right)\right) \left(1 - \exp\left(-\frac{\eta_T \bar{\gamma}}{4}\right)\right)^{M-1} \right\}. \end{aligned} \quad (16b)$$

Note that (16a) corrects [2, eq. (29)] and (16b) is equal to [2, eq. (16)], as expected. Note that the BER can be obtained from the SER using  $P_b(E) = \frac{M}{2(M-1)} P_s(E)$  [2].

### C. Theoretical and Simulation Results

Fig. 6 shows the BER of MFSK as a function of average SNR per bit per branch for postdetection SSC with  $M=2$  and 4 over i.i.d Rician fading with  $K=5$  obtained from Monte Carlo simulations and from the theoretical results in (16) and in [1, eq. (29)]. Fig. 6 confirms the validity of our theoretical result given in (16) and also shows that the analytical expression given in [2, eq. (29)] overestimates the performance. For example, at a BER of  $10^{-3}$  the SNR difference between the correct and the incorrect result is 0.94 dB and 1.11 dB for  $M=2$  and  $M=4$ , respectively.

Fig. 7 shows the average BER of noncoherent QFSK over i.i.d Rician fading as a function of normalized switching threshold for  $K=3$  and for several values of average SNR. The optimum switching thresholds are clearly indicated in the figure. Note that as the average SNR increases the optimal switching threshold decreases.

Fig. 8 shows the BER performance of noncoherent QFSK with predetection SSC and postdetection SSC in Rician fading for  $K=2, 4$  and 6. Fig. 8 indicates that the SNR difference between predetection SSC and postdetection SSC slightly increases as the fading severity is decreased. For example, at a BER of  $10^{-3}$  the SNR difference between predetection SSC and postdetection SSC is 0.63 dB and 0.70 dB, for  $K=2$  and  $K=6$ , respectively. Fig. 8 also shows that the performance difference between predetection SSC and postdetection SSC is much less than that reported in [2]. For example, at a BER of  $10^{-4}$  and for  $K=4$  the SNR difference between predetection SSC and postdetection SSC is only 0.50 dB; however, using the results of [2] the SNR difference is predicted as 1.30 dB which shows an error of 0.80 dB in SNR difference.

### IV. CONCLUSION

In this paper, we have corrected previous results on the performance of BFSK and MFSK with dual-branch postdetection SSC in Rician fading channels. Analytical expressions were obtained for the BER of BFSK and MFSK with postdetection SSC and the results were verified by Monte Carlo simulations. Optimum switching thresholds were obtained for minimizing the BER. The BER performance of postdetection SSC was compared with the BER of predetection SSC in Rician fading and it was shown that although postdetection SSC outperforms predetection SSC for all values of SNR, previously reported results can overestimate the difference by several dBs in SNR.

### REFERENCES

- [1] M.-S. Alouini and M. K. Simon, "Postdetection Switched Combining- A Simple Diversity Scheme With Improved BER Performance," *IEEE Trans. Commun.*, vol. 51, pp. 1591–1602, Sept. 2003.
- [2] M. K. Simon and M.-S. Alouini, "Probability of Error for noncoherent M-ary orthogonal FSK With Post-detection Switched Combining," *IEEE Trans. Commun.*, vol. 51, pp. 1456–1462, Sept. 2003.
- [3] G. L. Stuber, *Principles of Mobile Communication*, 2nd ed. Norwell, MA: Kluwer Academic Publishers, 2001.
- [4] M. K. Simon and M.-S. Alouini, *Digital Communication over Fading Channels: A Unified Approach to Performance Analysis*. New York: Wiley, 2000.
- [5] I. S. Gradshteyn and I. M. Ryzhik, *Table of Integrals, Series and Products*, 6th ed. San Diego, CA: Academic Press, 2000.

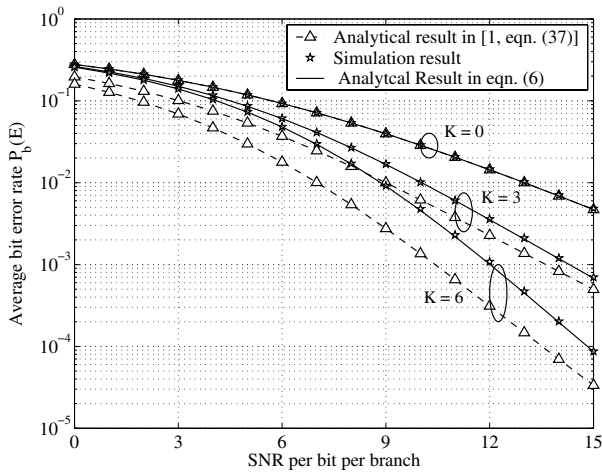


Fig. 3. The average BER of noncoherent BFSK with postdetection SSC versus SNR in i.i.d Rician fading for  $K = 0, 3$  and  $6$ .

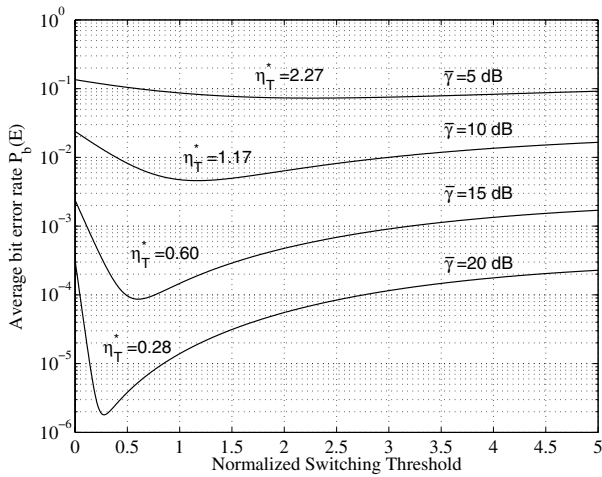


Fig. 4. The average BER of noncoherent BFSK in i.i.d Rician fading channels with postdetection SSC versus the normalized switching threshold for  $K = 6$  and  $\bar{\gamma} = 5, 10, 15$  and  $20$  dB.

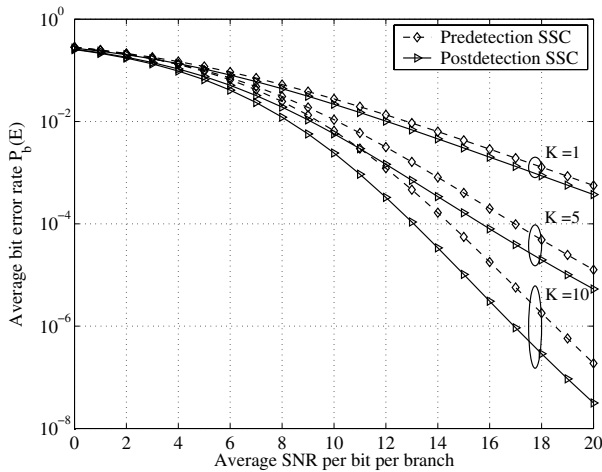


Fig. 5. Comparison of the average BER of noncoherent BFSK in i.i.d Rician fading with predetection and postdetection SSC for  $K = 1, 5$  and  $10$ .

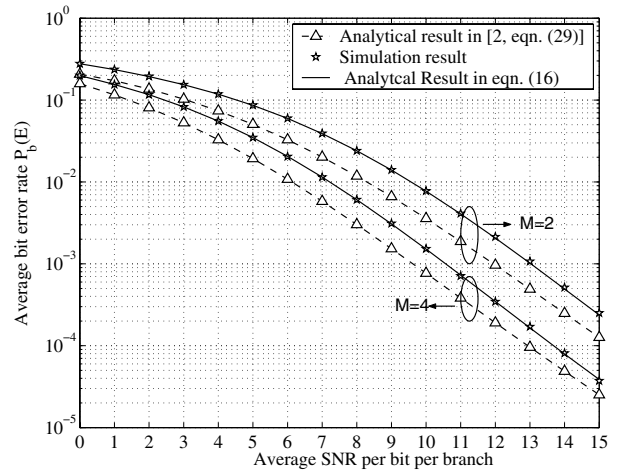


Fig. 6. The average BER of noncoherent  $M$ -ary FSK as a function of average SNR per bit per branch in i.i.d Rician fading with  $K = 5$  for  $M = 2, 4$ .

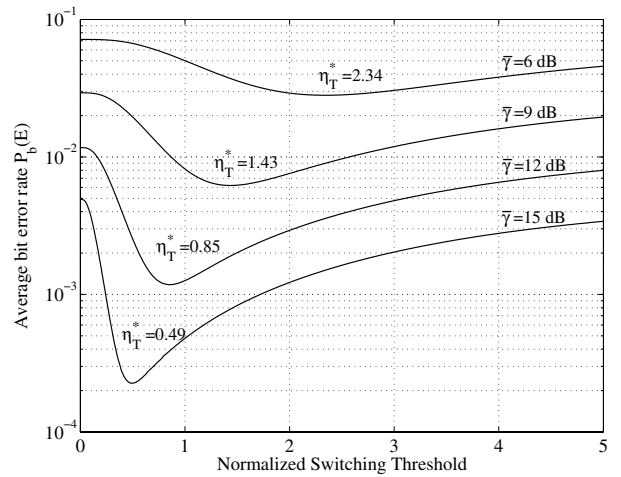


Fig. 7. The average BER of noncoherent QFSK over i.i.d Rician fading channels with postdetection SSC versus the normalized switching threshold for  $K = 3$  and  $\bar{\gamma} = 6, 9, 12$  and  $15$  dB.

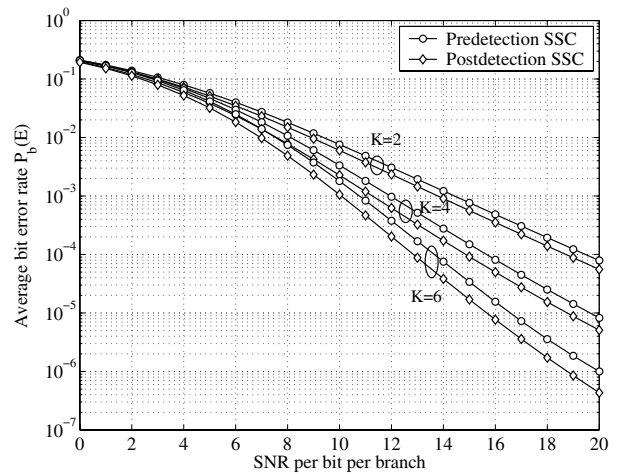


Fig. 8. The average BER of noncoherent QFSK with predetection and postdetection SSC in i.i.d Rician fading as a function of average SNR per bit per branch for  $K = 2, 4$  and  $6$ .